Genesis of the Gulf Stream Subseasonal Variability in the Florida Straits

Kandaga Pujiana[1,2], Denis Volkov[1,2], Shenfu Dong[2], Gustavo Goni[2], and Molly Baringer[2]

[1]University of Miami Cooperative Institute for Marine and Atmospheric Studies, Miami, United States.
[2]NOAA Atlantic Oceanographic and Meteorological Laboratory, Miami, United States.

Corresponding author: Kandaga Pujiana (kandaga.pujiana@noaa.gov)

Key Points:

- Subseasonal variability accounts for a substantial fraction of the Florida Current transport variance
- Coastal-trapped waves are the primary driver for the Florida Current subseasonal variability
- Alongshore wind-driven Ekman dynamics control the genesis of the subseasonal coastal-trapped waves

Abstract

The properties and generation mechanisms of the Florida Current subseasonal variability (20 – 100 days) are evaluated from in-situ and satellite observations. The Florida Current volume transport estimates from submarine cable measurements reveal that subseasonal variability accounts for 37% of the total transport variance. It is most active through September - November and marked by quasi-monthly variation. Here we show that coastal-trapped waves generated by alongshore winds off the southern Mid-Atlantic Bight coast are the primary driver of the Florida Current transport subseasonal variability. In contrast, the role of local winds is insignificant. The subseasonal coastal-trapped waves cover a waveguide from Cape May to Port Isabel within 15 days with an average phase speed of 2.5 ± 0.4 m s^{-1}. While transiting in the Florida Straits, the subseasonal waves modulate the Florida Current transport by up to 2.6 Sv, on average, close to the standard deviation of the total transport variability of 3.4 Sv. Under strong stratification in the Florida Straits, manifested in the Rossby deformation radius exceeding the cross-shelf length scale by a factor of 5, the waves exhibit Kelvin wave properties expected from theory. As the waves propagate into the Gulf of Mexico, their energy substantially dissipates. The wave amplitude at Cape May of up to 15 cm is five times higher than at Port Isabel.

Plain Language Summary

The Florida Current, an important constituent of the meridional overturning circulation in the subtropical North Atlantic, is crucial for the oceanic heat and freshwater transports and hence influences the regional weather and climate variations. Past studies show that the Florida Current exhibits changes with time scales that range from days to years. Our study attempts to elucidate the energetic subseasonal variability of the Florida Current with periods ranging from 20 to 100 days, whose characteristics and genesis have remained least understood. Based on the analyses of the most extensive in-situ and satellite measurements in the Florida Straits to date, we demonstrate that coastally trapped waves originating from the southern Mid-Atlantic Bight are the predominant driver of the Florida Current subseasonal variability. The alongshore wind-forced subseasonal waves modulate the Florida Current transport by a substantial amount, comparable to the standard deviation of the total transport variability. The far-reaching impacts of the waves on sea level along the United States East and Gulf Coast are discussed.

1. Introduction

The Florida Current (FC), the headwaters of the Gulf Stream, is an important component of the meridional overturning circulation in the subtropical North Atlantic. It is a highly variable, surface-intensified flow, with variations spanning across a broad range of timescales from days to years [e.g., *Beal et al.*, 2008; *Lee et al.*, 1985; *Meinen et al.*, 2010; *Schott et al.*, 1986]. The FC has been monitored nearly continuously since 1982 using a submarine telephone cable between Florida and the Bahamas (inset of Fig. 1) [e.g., *Baringer and Larsen*, 2001]. Calibrated with direct ocean current velocity measurements from Pegasus and dropsonde profilers, the cable voltages yield the daily time series of the FC volume transport [*Garcia and Meinen*, 2014]. The long-term average cable-derived transport is 31.8 ± 3.4 Sv [1Sv = 10^6 m^3s^{-1}; *Baringer and Larsen*, 2001; *Larsen and Smith*, 1992; *Meinen et al.*, 2010], which is close to the transport estimates obtained using other measurement techniques in the vicinity of the cable [*Lee et al.*, 1985; *Molinari et al.*, 1985].

About 30% of the observed FC transport variance is attributable to processes with a climate-relevant timescale range between seasonal and longer periods [e.g., *Meinen et al.*, 2010]. The seasonal cycle of the FC transport exhibits a maximum in July, followed by a quick drop to a minimum in November - December, with a peak-to-peak range of 4 - 5 Sv sporadically changing with time [*Baringer and Larsen*, 2001; *Larsen and Smith*, 1992; *Rosenfeld et al.*, 1989]. The driving mechanisms of the seasonal cycle have been attributed to barotropic processes in response to winds prevailing either locally in the Florida Straits or off the Northeast coast of America. The solutions of a wind-forced response model indicate that the seasonal cycle of the FC is a barotropic response to the along-stream winds within the Straits [*Lee and Williams*, 1988]. In contrast, the results of an adjoint model link the annual cycle to wind-forced barotropic waves originating along the Northeast American coast [*Czeschel et al.*, 2012]. As for the year-to-year change of the FC transport, *Domingues et al*. [2016] proposed long baroclinic Rossby waves originating in the eastern North Atlantic as a mechanism modulating the FC seasonal change. *DiNezio et al.* [2008] suggested a similar FC transport interannual variability source.

The majority of the observed FC transport variance lies between the tidal and seasonal periods with amplitudes comparable to or greater than the seasonal cycle [*Meinen et al.*, 2010; *Mooers et al.*, 2005; *Schott et al.*, 1988]. Many studies have reported a variety of processes governing the FC transport variability on synoptic or weather timescales from a few to 15 days [e.g., *Johns and Schott*, 1987; *Lee and Williams*, 1988]. Synoptic-scale winds over the Florida Straits, which are more energetic during winter than summer, contribute substantially to force the 4 - 10 day variations of the FC transport [*Schott et al.*, 1988]. Synoptic changes in the FC often reflect a geostrophic response to the sea level gradient change across the Florida Straits. They derive from the convergence of cross-strait current driven by synoptic along-strait winds via Ekman dynamics [*Lee and Williams*, 1988]. As for the 10 - 15-day periods, the FC is dominated by northward propagating features reminiscent of meanders. Nevertheless, the impacts of meandering motions on the FC transport are limited as they predominantly project in the cross-strait direction [*Johns and Schott*, 1987].

The broad period range between the synoptic and seasonal timescales is the subseasonal or intraseasonal period band, which conventionally encompasses a range of periods between 20 - 100 days [e.g., *Zhang*, 2005; *Maloney et al*., 2008]. The cable voltage-inferred FC transport exhibits energetic variability within the subseasonal period band. Using a record between 1982 - 1998, *Meinen et al*. [2010] showed that 46% of the FC transport variance is attributable to the variability between 1-to-11 months. *Volkov et al.* [2020] demonstrated that the FC transport varying between 20 - 170 days estimated from altimetry during 2005 - 2020 exhibits a standard deviation of 2.4 Sv, which is the largest compared to that for the seasonal and interannual period bands.

Despite its substantial contribution to the highly variable FC [*Meinen et al.*, 2010], the evolution and genesis of subseasonal variability in the Florida Straits remain poorly understood. *Schott et al.* [1988] attempted to analyze the FC subseasonal variability based on ocean current velocities from an array of moorings across the Florida Straits near the submarine cable during April 1982 - June 1984. They reported a correlation between the FC volume transport and local winds on subseasonal timescales. They argued that a simple frictional flow model driven by the along-strait winds could explain the correlation, implying local winds as a likely source of the FC subseasonal variability.

Due to the key role in transporting heat, freshwater, and nutrients, it is critical to improving our understanding of the FC variations at a wide range of timescales. This study builds upon previous investigations to evaluate the characteristics and driving mechanisms of the FC transport subseasonal variability in terms of coastal-trapped wave theory. To assess the subseasonal characteristics of the FC transport, we utilize the most extensive observations to date in the Florida Straits, including those from the submarine cable and bottom pressure recorders. Sea level anomalies from tide gauges on the United States [U.S.] East and Gulf Coast, with satellite-retrieved oceanic and atmospheric parameters over the North Atlantic, are used to monitor non-local sources of the FC transport on subseasonal timescales.

This manuscript is organized as follows. In section 2, we describe the data and methods. In section 3, we discuss the main properties of subseasonal variability in the oceanic parameters observed in the Florida Straits and how they relate to local winds. Then we proceed with assessments of subseasonal characteristics of the sea level anomaly data from tide gauges in section 4, including analyses of coastal-trapped wave properties. Section 5 examines the basin-scale structure and genesis of the subseasonal coastal-trapped waves. A discussion (section 6) and conclusions (section 7) follow.

2. Data and Methods

The daily, quasi-continuous volume transport estimates from the undersea telephone cable in the Florida Straits at 27ºN (red line in the inset of Fig. 1) from 1982 to present are the primary data from which we derived the inferences for the FC transport subseasonal variability. These estimates are reasonably close to those obtained from repeated shipboard Pegasus, dropsonde, and lowered Acoustic Doppler Current Profiler (LADCP) casts in the vicinity of the cable site (rectangles in the inset of Fig. 1), particularly those observed after the beginning of the new millennium [*Meinen et al.*, 2021]. Despite showing an overall good agreement with the shipborne measurements, the accuracy of the cable's estimates was relatively low between 1993 - 1998, when the cable was in active use for telecommunication services [Larsen, 1991; Volkov, 2020]. Following this period, there was a 17-month data gap in the cable record. Therefore, we examined the FC transport estimates from the cable voltage measurements between 2001 - 2019. A three-day low pass filter was applied to remove the tidal and magnetic field variations from the daily transport estimates [*Meinen et al.*, 2010].

Complementing the transport estimates from cable measurements, we also used the FC transport inferred from satellite altimetry [*Volkov et al.*, 2020] and repeated ship sections between 2001 - 2019. During this time interval, 116 dropsonde and 80 LADCP sections were conducted across the FC at 27ºN. At each of the nine stations in the Florida Straits, dropsondes measure the vertically-averaged horizontal current velocity, whereas the LADCP casts yield the vertical structure of the velocity. For details of the ship sections, readers are referred to *Garcia and Meinen* [2014]. A subset of the FC transport time series is shown in Figure 2a.

The shipboard surveys across the Florida Straits at 27ºN also included Conductivity-Temperature-Depth (CTD), and eXpendable BathyThermographs (XBT) deployments, with the former measuring profiles of both temperature (T) and salinity (S), while the latter profiling T only. The World Ocean Atlas 2013 (WOA2013) salinity product was used to supplement T from the XBT deployments. We focused on the subsurface T and corresponding Brunt-Väisällä frequency (N) profiles for this study, helpful in assessing the subseasonal coastal-trapped wave properties, including their vertical and cross-shelf scales. The Brunt-Väisällä or stratification frequency was determined from the observed potential density (ρ) profiles, which is expressed as $N^2 \equiv \frac{-g}{\rho_0}\frac{d\rho}{dz}$, where ρ was determined from T and S, ρ_0 is the background density structure inferred from the time-averaged ρ, z is the vertical coordinate, and g is the gravitational acceleration constant of 9.8 m s^{-2}.

Besides the FC transport estimates, we examined pressure data from two bottom pressure recorders (BPRs) deployed in shallow waters (~ 12 m) on the western and eastern sides of the Florida Straits at 27ºN (stars in the inset of Fig. 1; *Meinen et al*., 2021) to explore the subseasonal variability properties therein. We henceforth refer to pressure measured by the BPRs on the western and eastern sides of the straits as P_W and P_E, respectively. Although the BPRs have been operational since July 2008 and recording 5-minute averages of pressure data, for this study, we examined the daily averages of pressure records between July 2008 - September 2014 (Fig. 2b). It is the observational period during which both sensors were synchronously operational and recorded nearly continuous data. Similar to that applied to the cable's FC transport estimates, a three-day low-pass filter was used to remove tidal signals from the daily pressure records [*Meinen et al*., 2021].

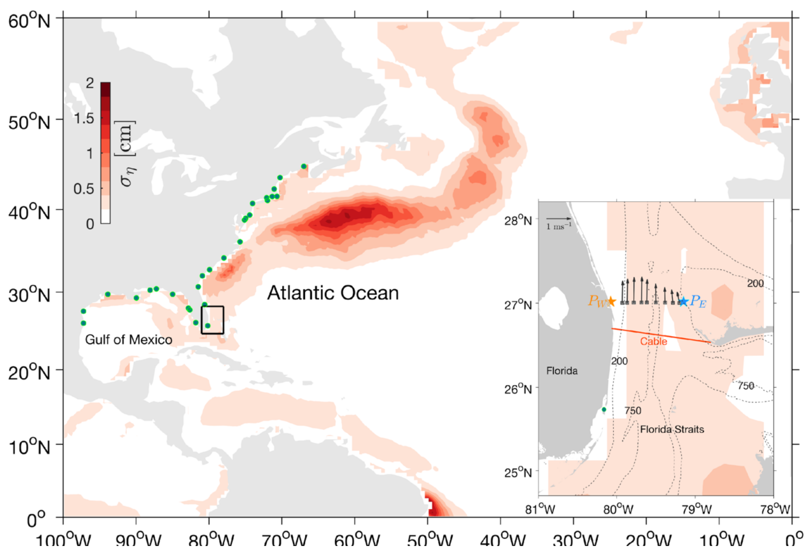

Figure 1. Standard deviation of the satellite-derived sea level anomaly (η; shading) in the subseasonal period band between 20 - 100 days in the North Atlantic. Green dots mark a network of tide gauges along the U.S. East and Gulf Coast. The inset illustrates locations of the observations in the Florida Straits, with stars marking bottom pressure recorders (BPRs), gray boxes denoting dropsonde, eXpendable BathyThermograph (XBT), and Conductivity-Temperature-Depth (CTD) casts, arrows indicating the vertical-mean of horizontal velocity averaged for all the casts between 2001 - 2019, and the red line showing submerged cable for monitoring the FC transport. Dashed contours indicate bottom depth.

In addition to the in-situ observations in the Florida Straits, we examined sea level anomaly (η) from a network of tide gauges along the U.S. East and Gulf Coast (green dots in Fig. 1), and satellite-derived wind stress (τ) and η data over the North Atlantic to gain insights into non-local processes driving the FC subseasonal variability and their basin-scale structures. We examined a research quality data set of daily coastal η at the tide gauges between 2001 - 2019 provided by the University of Hawaii Sea Level Center (UHSLC) [*Caldwell et al*., 2015]. As for the satellite data, we employed the daily, 0.25° latitude x 0.25° longitude gridded τ and η data for the 2001 - 2019 period from the Copernicus Marine and Environment Monitoring Service (CMEMS) products.

A number of time series and spatial analysis methods were applied to the in-situ and satellite data. We analyzed the 20 - 100 day band-pass filtered data to assess the spatial structures of the subseasonal mode using a Complex Empirical Orthogonal Function (CEOF) analysis and a linear regression method [*Thomson and Emery*, 2014]. Isolating the variability of the subseasonal and other frequency bands was achieved using a fourth-order band-pass Butterworth filter. Any data gaps were filled with a simple linear interpolation. To estimate the alongshore wavenumbers of subseasonal coastal-trapped waves, we applied a coherence analysis [*Percival and Walden*, 1993] to the coastal η data from multiple pairs of tide gauges. Based on the phase lags determined from the coherence analysis, we derived the wavenumbers which then were used to estimate the dispersion relation of the subseasonal mode.

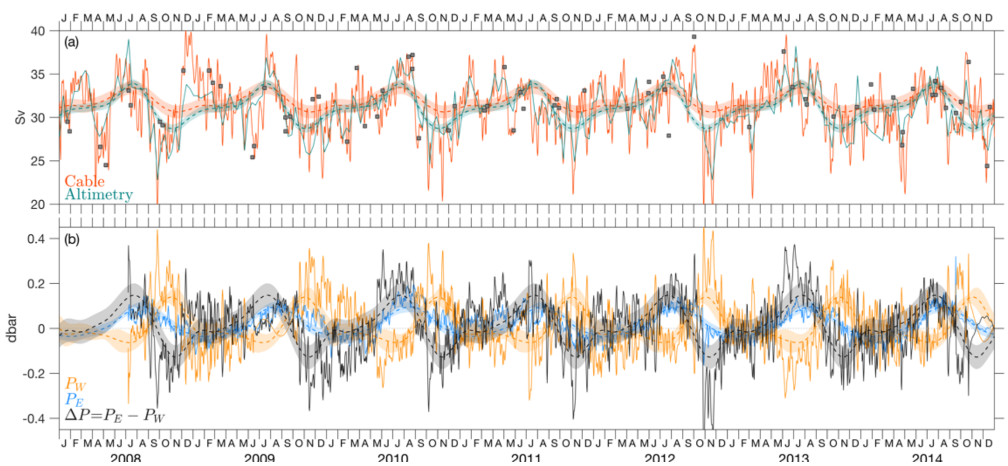

Figure 2. (a) A subset of the FC volume transport time series estimated from cable voltages [red], satellite altimetry [green], and shipboard measurements (dropsondes and LADCP) [rectangles]. (b) Time series of pressure data from the BPRs deployed on the west side [P_W; orange] and east side [P_E; blue] of the Florida Straits. The black curve indicates the across-channel or cross-stream pressure difference [$\Delta P = P_E - P_W$]. The color-coded dashed curves denote the seasonal cycles attributable to the time series, with shades indicating the 95% bootstrap confidence limits of the cycles.

3. Statistics of subseasonal variability in the Florida Straits

Consistent with the results reported in past studies, the FC volume transport inferred from cable voltages reveals large variations about its poleward transport, with the mean and standard deviation values of 31.6 ± 3.3 Sv for the entire record analyzed herein between 2001 - 2019 and of 31.1 ± 3.4 Sv for the subset throughout 2008 - 2014 as shown in Figure 2a. For comparison, the mean and standard deviation estimates from altimetry are 31.2 ± 2.8 Sv during 2001 - 2019 and 31.0 ± 2.8 Sv during 2008 - 2014. Ubiquitous subseasonal and synoptic variations characterize the daily FC transport estimates (Fig. 2a), modulating year-to-year changes of the transport seasonality [*Meinen et al.*, 2010; *Meinen et al.*, 2021]. The pronounced subseasonal fluctuations emphasize the need for long-term observations in the Florida Straits to resolve any changes in the seasonal cycle of the FC transport.

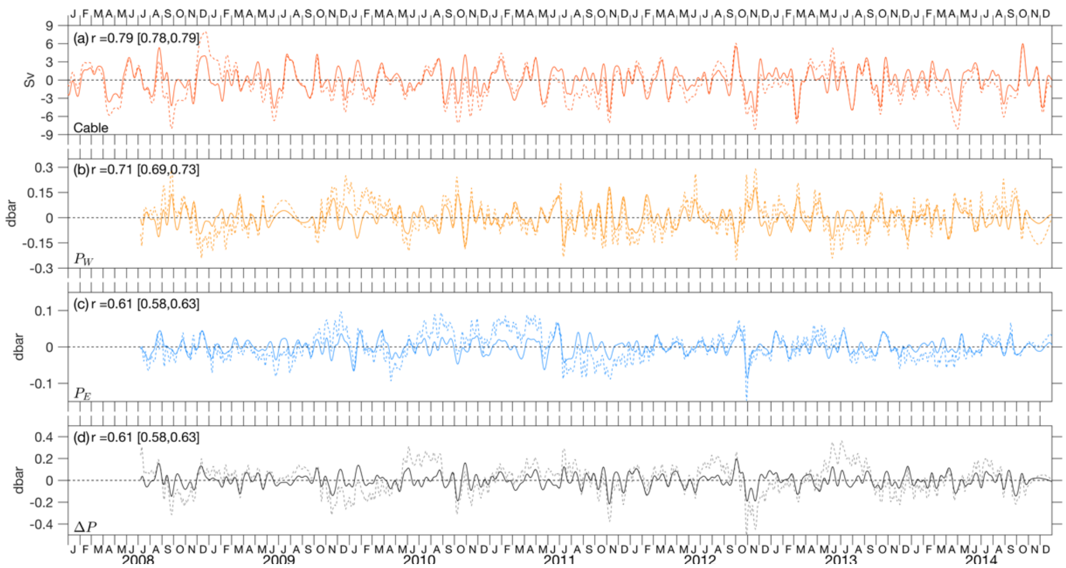

Figure 3. Time series of the subseasonal (solid) and 20-day low-pass filtered anomalies (seasonal cycle removed; dashed) of (a) the FC transport from cable voltages, (b) P_W, (c) P_E, and ΔP in the Florida Straits. The correlation coefficient, *r*, indicates the degree of correlation between the solid and dashed curves. The values within the bracket denote the 95% confidence interval for the correlation coefficient.

A quasi-monthly oscillation, marked with a spectral peak centered at about 35 days (not shown), predominantly accounts for the FC transport subseasonal variability observed during 2001 - 2019, while oscillations every 2-3 months prevail in some years, including between 2008 - 2014, as shown in Figure 3a. The standard deviation of the FC transport variability on subseasonal timescales observed between 2001 - 2019 from the cable is 1.7 ± 0.02 Sv, slightly larger than that from altimetry, 1.5 ± 0.07 Sv. However, *Schott et al.* [1988], based on earlier observations of moored current meter arrays between 1982 - 1984 in the Florida Straits, revealed a rather red spectrum of the FC transport across the resolved frequencies, indicative of no particular dominant frequency within the subseasonal frequency band. The discrepancy may stem from less active subseasonal variability occurring in that particular period reported in their study. Intermittent subseasonal signature is not atypical in oceanic and atmospheric processes [*Lau and Walliser*, 2011]. Indeed, the voltage-derived FC transport confirms a much weaker quasi-monthly variation (not shown) and an overall smaller standard deviation, 1.5 ± 0.05 Sv, for the subseasonal variability during 1982 - 1984.

The subseasonal period band contains a significant fraction of the total variance of the FC transport variability. The total variance during 2001 - 2019 is 10.7 Sv^2, with the subset between 2008 - 2014 exhibiting a larger value of 11.6 Sv^2. Of the total FC transport variability, about 37% of the variance is attributable to subseasonal variability for the entire data or the subset. It is higher than the total percentage of the synoptic (3 - 15 days), seasonal (11 - 13 months), and interannual variances (13 - 42 months), which are 25%, 2%, and 8%, respectively.

Relative to the 20-day low-pass filtered FC transport anomalies (seasonal cycle removed), subseasonal variability accounts for 67% of the transport anomalies during 2008 - 2014 (Fig. 3a). The percentage slightly drops to 62% when considering the entire data between 2001 - 2019.

Subseasonal variability constitutes a significant fraction of the total pressure variance in the Florida Straits. The total percentage of subseasonal variance for P_W and P_E is 24% and 16%, respectively, comparable to or higher than the total percentage of the synoptic and seasonal variances. Moreover, subseasonal variability exhibits a notable contribution to the 20-day low-pass filtered pressure anomalies. It accounts for 50% and 37% of the total variance of the low-pass filtered P_W and P_E anomalies, respectively (Figs. 3b-d). The discrepancy in the percentage confirms a more energetic subseasonal signature on the west side of the Florida Straits. The seasonal cycle was removed from the 20-day low-pass filtered pressure time series as in the FC transport.

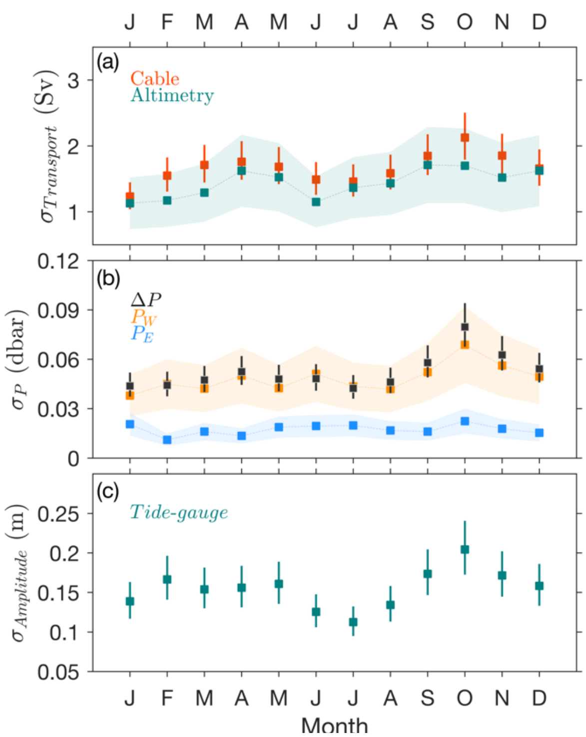

Figure 4. The seasonal cycle of the standard deviation of (a) the FC transport estimates, (b) the bottom pressure records in the Florida Straits, and (c) the principal component of the leading CEOF mode of the subseasonal η variability at tide gauges along the U.S. East and Gulf Coast between Cape May and Apalachicola. Color-coded shadings or vertical lines denote 95% bootstrap confidence limits. The standard deviations observed between 2001 - 2019 are used to determine the seasonal cycle for the FC transport and the tide gauge η data, while those throughout July 2008 - September 2014 are employed for the bottom pressure data.

Based on the seasonal cycle of the standard deviation of the FC transport and bottom pressure subseasonal variations, we argue that subseasonal variability in the Florida Straits exhibits seasonality. The monthly climatology of the standard deviation indicates that the FC transport subseasonal variation is more active during September - November, and peaks in October (Fig. 4a). A more energetic subseasonal variability in autumn is consistently observed in the FC transport estimates from both the cable and altimetry. Similar to the transport estimates, the pressure on the west side and the cross-stream pressure gradient on subseasonal timescales demonstrate a maximum standard deviation in October (Fig. 4b).

Besides being most active in boreal autumn, the FC transport and the bottom pressure on subseasonal timescales are statistically correlated. The FC transport is correlated with ΔP, with a correlation coefficient $r = 0.71$ (0.69, 0.73), where the values in the bracket represent 95% confidence limits. When only the autumn months data are considered, the r-value increases to 0.84 (0.81, 0.87). The correlation suggests that a linear relationship between the pressure difference and the FC transport would explain about 50% (70% for the autumn data) of the FC transport variance for the subseasonal band. Moreover, it indicates that a geostrophic balance between the FC and the cross-stream pressure gradient holds for subseasonal timescales. The pressure on the western side of the Florida Straits dominates the subseasonal geostrophic FC variability, with about 41% (70% for the autumn time series) of the FC transport subseasonal variance being accounted for by P_W. Meanwhile, P_E accounts for only 16% of the FC transport subseasonal variance even when solely based on the autumn data.

To trace energy sources for the subseasonal variations of the FC transport estimates and the pressure records, we first review the potential impact of local winds on the Florida Straits. *Schott et al.* [1988], using two-year-long transport estimates from an array of current meters deployed in the vicinity of the cable, argued that the FC transport subseasonal variability is primarily caused by local winds. However, our assessment employing longer transport estimates indicates that local winds are unlikely a major factor in driving the FC subseasonal variability. Neither the wind stress components nor the wind curl ($\nabla \times \tau$) is strongly correlated with the FC transport and bottom pressure on subseasonal timescales. The meridional wind stress (τ^y) demonstrates the largest correlation with both the FC transport [$r = 0.21$ (0.16, 0.23)] and ΔP [$r = 0.28$ (0.22, 0.30)], with τ^y leading by 1 - 2 days. As both the FC transport and the pressure gradient show a weak positive correlation with τ^y, a balance between wind stress and frictional dissipation in the along-stream direction is not a predominant factor in explaining the subseasonal variability in the FC transport. Other wind components such as the zonal wind stress (τ^x) and wind stress curl show weaker correlations. Given its weak correlations with local winds, the FC transport likely derives most of its subseasonal energy from remote processes.

4. Subseasonal coastal-trapped wave properties and impacts on the FC transport

The weak correlation of local winds with the FC volume transport and the bottom pressure indicates remote forcing as a driving mechanism for the observed subseasonal variability in the Florida Straits. We examined sea level anomaly within the continental shelf region along the U.S. East and Gulf Coast to identify a plausible remote driver.

On subseasonal timescales, the largest correlation between the FC transport and sea level anomaly appears to be confined within the continental shelf of the South Atlantic Bight, with the outer shelf edge marked by an isobath of 200 m (Fig. 5a). An inverse relationship pattern between the FC transport and satellite η appears relatively continuous across the continental shelf between Duck Pier and Virginia Key. However, it is patchy both farther north along the U.S.

East Coast and farther west along the Gulf Coast. It corroborates the observed inverse relationship between the FC transport and the bottom pressure P_W on subseasonal timescales.

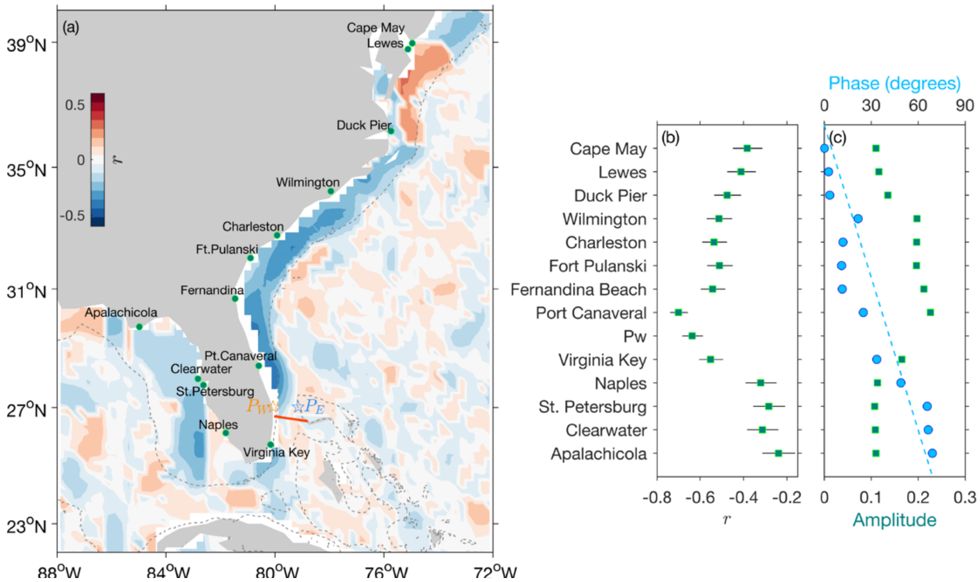

Figure 5. Lagged correlation coefficient [*r*] values between the FC transport and η on subseasonal timescales observed from (a) altimetry and (b) tide gauges along the coast between Cape May and Apalachicola [green dots]. The *r*-value at each grid or tide gauge is the maximum value identifiable at the time lags between -50 and +50 days. The dashed contours mark the 200-m isobath. The horizontal lines in (b) indicate the correlation coefficient's 95% bootstrap confidence limits. (c) The amplitude (green) and phase (blue) of the leading CEOF mode of subseasonal η at tide gauges shown by green dots in (a), with the real part of the CEOF mode representing the amplitude. The blue dashed line in (c) denotes the linear least-squares fit to the leading CEOF mode amplitude.

Similar to the altimetry data, coastal sea level anomaly at tide gauges from Cape May to Apalachicola demonstrates an inverse relationship with the FC transport on subseasonal timescales (Fig. 5b). The absolute value of the time-lagged correlation coefficients between the FC transport and the coastal η for the subseasonal period band is maximum at Port Canaveral, a nearby tide gauge station to the north of the cable site. It is within the error limits of the maximum correlation between subseasonal *PW* and subseasonal FC transport (Fig. 5b).

On subseasonal timescales, the FC transport lags the coastal η data at tide gauges north of the cable but leads those to the south, indicating propagation into the Gulf of Mexico. It takes about three days for subseasonal signals to propagate from Cape May to the Florida Straits and about eight days more to reach Apalachicola. Despite being statistically significant (*p* values are smaller than the significance level), the correlation at other tide gauges north of Cape May and west of Apalachicola is weaker (r < 0.2). Thus, the rest of the analysis is focused on the coastal η data at the tide gauges between Cape May and Apalachicola.

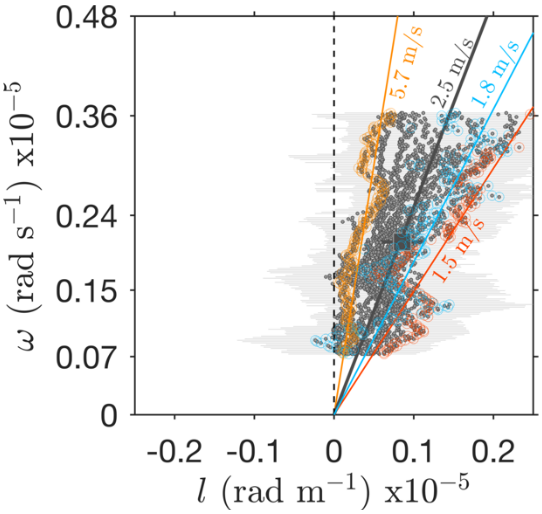

Figure 6. Observed frequency-wavenumber pairs (gray dots; ω - *l*) for the subseasonal period band, inferred from a coherence analysis of η at tide gauges (green dots in Fig. 5a). Positive values of *l* indicate phase propagation towards the Gulf of Mexico. Shades indicate the 95% confidence interval based on a Monte Carlo method. Orange, red, and blue dots denote the dispersion diagrams inferred from η at Cape May and Virginia Key, Virginia Key and Saint Petersburg, and Port Canaveral and Virginia Key, respectively. The color-coded lines demonstrate the linear least-squares fit to the dispersion diagrams.

As discussed above, the FC transport shows a statistically significant correlation with coastal sea level anomaly for the subseasonal period band, particularly between Cape May and Apalachicola, with the corresponding time lag suggestive of along the coast propagation into the Gulf of Mexico. Further analysis of the coastal η data indicates that the propagating feature can be interpreted in terms of coastally trapped wave properties. A wave inference we deduced is the dispersion relation, which was obtained from a coherence analysis of the η data from multiple pairs of tide gauges separated by a distance (*d*) along the coast, resulting in a set of coherence amplitude and phase (α) estimates at a discrete set of frequencies (*ω*). Considering only the phase information when the respective coherence amplitude exceeds the 95% significance level, we determined the horizontal wavenumber as $l(\omega) = \frac{\alpha(\omega)}{d}$ for the subseasonal frequency band and subsequently the horizontal dispersion relation (*ω* - *l*), with positive *l* values denoting the horizontal wavenumber along the coast pointed towards the U.S. Gulf Coast.

The observed *ω* - *l* scatter generally clusters around the theoretical dispersion curve for Kelvin wave (Fig. 6), whose dispersion relation in the alongshore direction can be represented from theory as

$$\omega = l\,c, \qquad (1)$$

with *c* denoting the Kelvin wave phase speed. The least-squares fit (black curve in Fig. 6), inferred from fitting (1) to the observed *ω* - *l*, yields a *c* value of 2.5 ± 0.4 m s^{-1}. Most of the observed alongshore wavenumber values exceed zero ($l > 0$), confirming predominant propagation into the Gulf of Mexico on subseasonal timescales.

Interestingly, the dispersion diagrams determined from the subseasonal component of the coastal η data along the U.S. East Coast yield a faster phase speed estimate than those along the Gulf Coast. For example, the dispersion diagram derived from the η data at the Cape May and Virginia Key pair (orange circles in Fig. 6) yields a c estimate over two times larger than that inferred from the Virginia Key - Saint Petersburg pair (red circles in Fig. 6). The disparity in wave phase speeds remains unknown.

A reasonable agreement between the observed and analytical Kelvin wave dispersion relations might indicate that the properties of Kelvin waves could account for the subseasonal coastal-trapped waves identifiable from the observations. Of course, due to the actual sloping shelf region, the observed subseasonal waves are not pure coastal Kelvin waves which theoretically require a vertical sidewall. The agreement is likely a reflection of much smaller shelf-width scales than the baroclinic Rossby deformation radius, whereby a condition of the vertical side boundary for Kelvin waves is applicable.

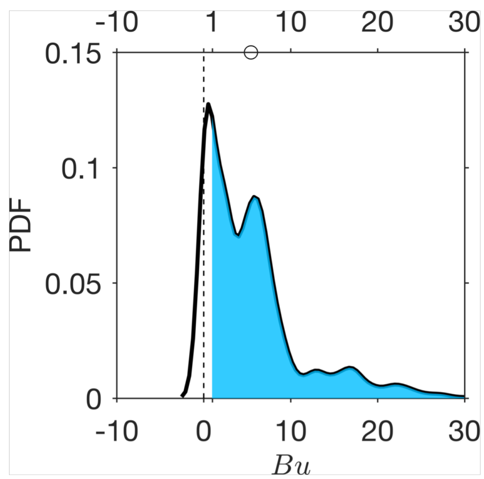

Figure 7. Distribution of the Burger number, *Bu*, values determined from the hydrographic and bathymetric data at the CTD and XBT stations in the Florida Straits at 27ºN during 2001 - 2019. Shaded area indicates values of $Bu > 1$, and the circle marks the average *Bu* value.

To gauge whether a vertical sidewall approximation is justified, we determined the ratio of the Rossby deformation radius over the cross-shelf scale of the topography, which can be approximately given as the Burger number

$$Bu = \left(\frac{NH}{\Omega L}\right)^2, \tag{2}$$

where N is the Brunt-Väisällä or buoyancy frequency, H is the vertical scale, Ω is the Coriolis parameter, and L is the cross-shelf length scale [*Cushman-Roisin and Beckers*, 2011]. The cross-shelf length scale is expressed as $L = h/|s|$, where h is the depth of the bottom topography and s is the offshore slope of h. Based on CTD and XBT measurements and bottom topography data in the Florida Straits at 27ºN, we argue that most Burger number estimates exceed one (Fig. 7). It substantiates that the off-shelf scale of a waveform propagating along the Florida coast follows that of the Rossby deformation radius and is larger than the cross-shelf length scale such that the wave may perceive the continental shelf and slope as a near-vertical sidewall.

The observed stratification frequency in the Florida Straits could provide insight into the phase speeds expected from Kelvin waves. For a given N, solving each baroclinic mode-n Kelvin wave $\frac{\partial}{\partial z}\left(\frac{1}{N^2}\frac{\partial \psi_n}{\partial z}\right) = \frac{\psi_n}{c_n^2}$ as an eigenvalue problem results in a phase speed estimate (c_n) and ψ_n for each mode, with ψ_n denoting the mode-n vertical structure function. Using the N profiles from the hydrographic observations in the Florida Straits at 27ºN, the c estimates for the first three gravest baroclinic modes are 1.8 ± 0.1 m s^{-1}, 0.8 ± 0.1 m s^{-1}, and 0.5 ± 0.1 m s^{-1}, respectively. The stratification-derived c estimate for the first baroclinic Kelvin wave mode reasonably approximates that from the subseasonal coastal η data at Port Canaveral and Virginia Key, whose ω - l diagram indicating an average phase speed of 1.8 ± 0.3 m s^{-1} along the East Florida coast for the subseasonal frequency band (blue dots and line in Fig. 6). Although composed of multiple baroclinic modes, the first baroclinic Kelvin wave mode is likely the dominant subseasonal coastal-trapped wave mode observed in the Florida Straits.

We applied a CEOF method to the subseasonal component of the η data at tide gauges between Cape May and Apalachicola to isolate the subseasonal coastal-trapped wave signals during 2001 - 2019. The leading CEOF mode of the η data accounts for 61% of the subseasonal variance and exhibits amplitudes generally increasing southward from Cape May to Port Canaveral and then decreasing in the Florida Straits and along the U.S. Gulf Coast (green boxes in Fig. 5c). It also captures the southward propagation of subseasonal η as its phase increases towards the Gulf of Mexico, indicative of the subseasonal mode first appearing along the U.S. East Coast before reaching the Gulf Coast, via the Florida Straits.

A linear least-squares fit to the CEOF phase at different tide gauges yields an average phase change of 1°/38 ± 3 km (dashed line in Fig. 5c). The phase change infers a phase speed of 2.4 - 2.8 m s^{-1} for subseasonal coastal-trapped waves along the U.S. East and Gulf Coast and recurring with a period of 30 days, which is within the confidence limits of the phase speed derived from the observed dispersion diagram. The results do not change when a similar analysis is applied to a merged dataset of the subseasonal variations of the coastal η and P_W data between July 2008 - September 2014.

A regression analysis between the leading complex principal component and the subseasonal variations of the coastal η and the FC transport and bottom pressure in the Florida Straits further highlights the evolution, transmission, and impacts of subseasonal coastal-trapped waves (Fig. 8). The regressed η attributed to a positive one standard deviation of the principal component clearly illustrates the propagation of a coastal-trapped wave crest from the U.S. East Coast to the Gulf Coast (Fig. 8a). The wave peak transmits from Cape May to Virginia Key within three and a half days, covering a distance of about 1675 km following the 200-m isobath, equivalent to a wave phase speed of 5.3 m s^{-1}. Along the West Florida Shelf coast from Virginia Key to Apalachicola, with a shorter distance of roughly 530 km between the two tide gauges, it propagates with a slower phase speed of 1.5 m s^{-1}. The phase speeds approximate those derived from the observed dispersion relation (Fig. 6).

Besides transmission, the regressed η showcases the evolution of the amplitude of subseasonal coastal-trapped waves as they dissipate towards the U.S. Gulf Coast. The wave peak amplitude is up to 5 cm at Port Canaveral and gradually decays to 2 cm at Apalachicola as the wave propagates into the Gulf of Mexico (Fig. 8a).

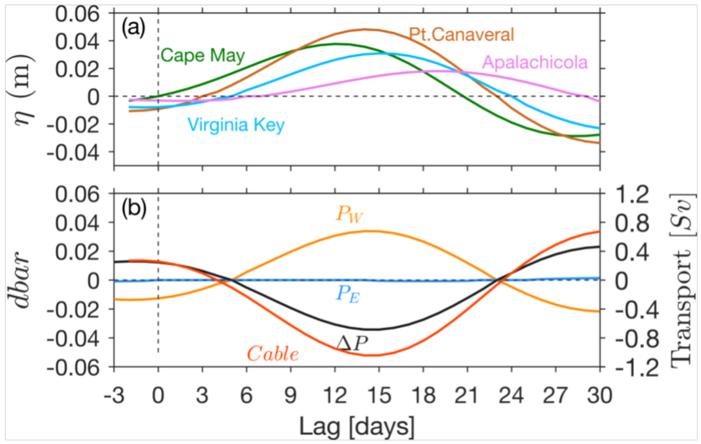

Figure 8. Time-evolution of the subseasonal time series of (a) coastal η at some select tide gauges along the U.S. East and Gulf Coast and (b) the FC transport [red curve] and bottom pressure in the Florida Straits, regressed against the principal component of the leading CEOF mode of the subseasonal coastal η data at tide gauges shown in Figure 5a. The regressed time series are scaled to one standard deviation of the principal component. Lag 0 marks when η = 0 and the rate of change of η is positive at Cape May.

In the Florida Straits, subseasonal coastal trapped wave crests reduce the cross-stream pressure gradient and the FC transport by up to 0.035 dbar (3.5 cm) and 1 Sv, respectively (Fig. 8b). A change in the transport of 1 Sv exerted by the subseasonal waves with an amplitude of about 5 cm at Port Canaveral is significant. This change represents 30% of the standard deviation of the total FC transport variability, which is about 3.4 Sv [*Meinen et al.*, 2010]. On the contrary, the subseasonal wave troughs increase the transport and pressure gradient.

The change in P_W controls the pressure gradient response to subseasonal wave passage in the Florida Straits, while P_E shows a lack of change (Fig. 8b). A more pronounced response in P_W than in P_E may reflect the wave's narrow cross-shelf scale relative to the distance between the two pressure recorders. The theoretical Kelvin wave solution for southward moving coastal-trapped waves in the Florida Straits at 27ºN signifies a zonal structure of pressure that exponentially decays with distance to the east. It can be presented as $P\ (x)\ = P_0 e^{\frac{-fx}{c}} cos(ly - \omega t)$, where x and y indicate the distance in the across- and along-strait direction, respectively, and P_0 is the pressure at $x = 0$ or the westernmost of the Florida Straits. Given $x = 80$ km (the nominal zonal distance between the BPRs), $c = 1.8$ m s^{-1} (the phase speed of the first baroclinic Kelvin wave mode estimated from a normal mode decomposition of the observed stratification at 27ºN), and assume $P_0 = P_W$, the estimated P_E is a twentieth of P_W. Thus, the insignificant change observed in P_E (blue curve in Fig. 8b) may reflect the across-strait structure of Kelvin wave, with a decay scale a third of the width of the Florida Straits at 27°N.

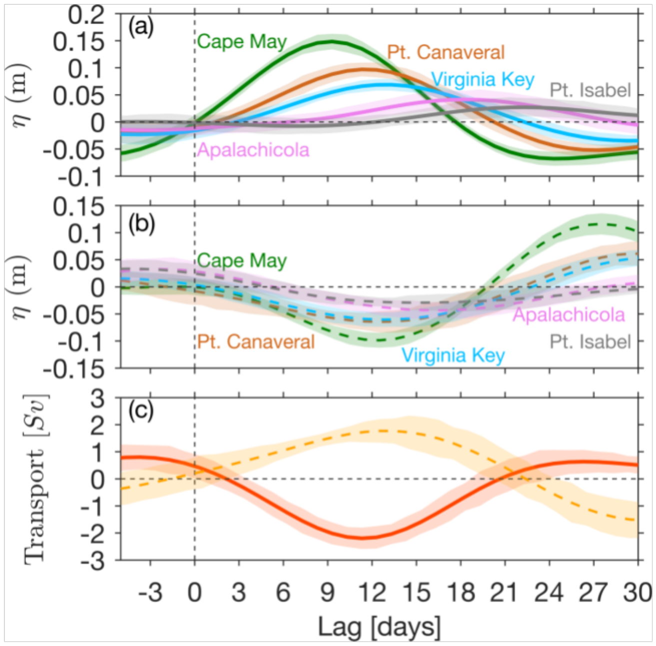

Figure 9. Composites of the subseasonal variations of coastal η (a and b) at some tide gauges along the U.S. East and Gulf Coast and the FC transport (c) attributed to extreme subseasonal coastal-trapped wave events during 2001 - 2019. (a) illustrates the composites for the downwelling events, while (b) demonstrates the composites for the upwelling events. Lag 0 marks when η = 0 and the rate of change of η is positive at Cape May.

To assess changes to coastal sea level anomaly and the FC transport due to more energetic subseasonal coastal-trapped waves, we defined the principal component values above and lower than the +2 and -2 standard deviation values as extreme events. There are 32 peaks for the positive standard deviation threshold value and 21 troughs for the negative threshold throughout the observation. We henceforth refer to the peaks and troughs as downwelling and upwelling events, respectively.

Composites of the subseasonal η data associated with the extreme events indicate that subseasonal coastal-trapped waves may modulate sea level anomaly at Cape May and Port Canaveral with an average amplitude varying between 10 - 15 cm for the downwelling events and 5 - 10 cm for the upwelling events, respectively (Fig. 9a and b). The wave crest or trough cycle is about 35 days at each tide gauge. It takes roughly 15 days for the subseasonal waves to transmit from Cape May to Port Isabel. However, the wave pulse is barely different from zero at the southwesternmost tide gauge on the U.S. Gulf Coast. In response to the extreme subseasonal waves, the FC transport registers an average change of 2.6 Sv and 2.0 Sv for the downwelling and upwelling events, respectively (Fig. 9c).

Similar to the subseasonal variations of the FC transport and the bottom pressure in the Florida Straits, subseasonal η at tide gauges between Cape May and Apalachicola reveals a seasonal pattern. The standard deviation of the principal component of the first CEOF mode of the subseasonal η data indicates that its average value for October is the largest relative to the average values for other months (Fig. 4c). Together with other results discussed above, the seasonality of subseasonal η provides another indicator of a causal relationship between the subseasonal coastal-trapped waves and the FC transport.

5. Basin-scale structure of subseasonal coastal-trapped waves

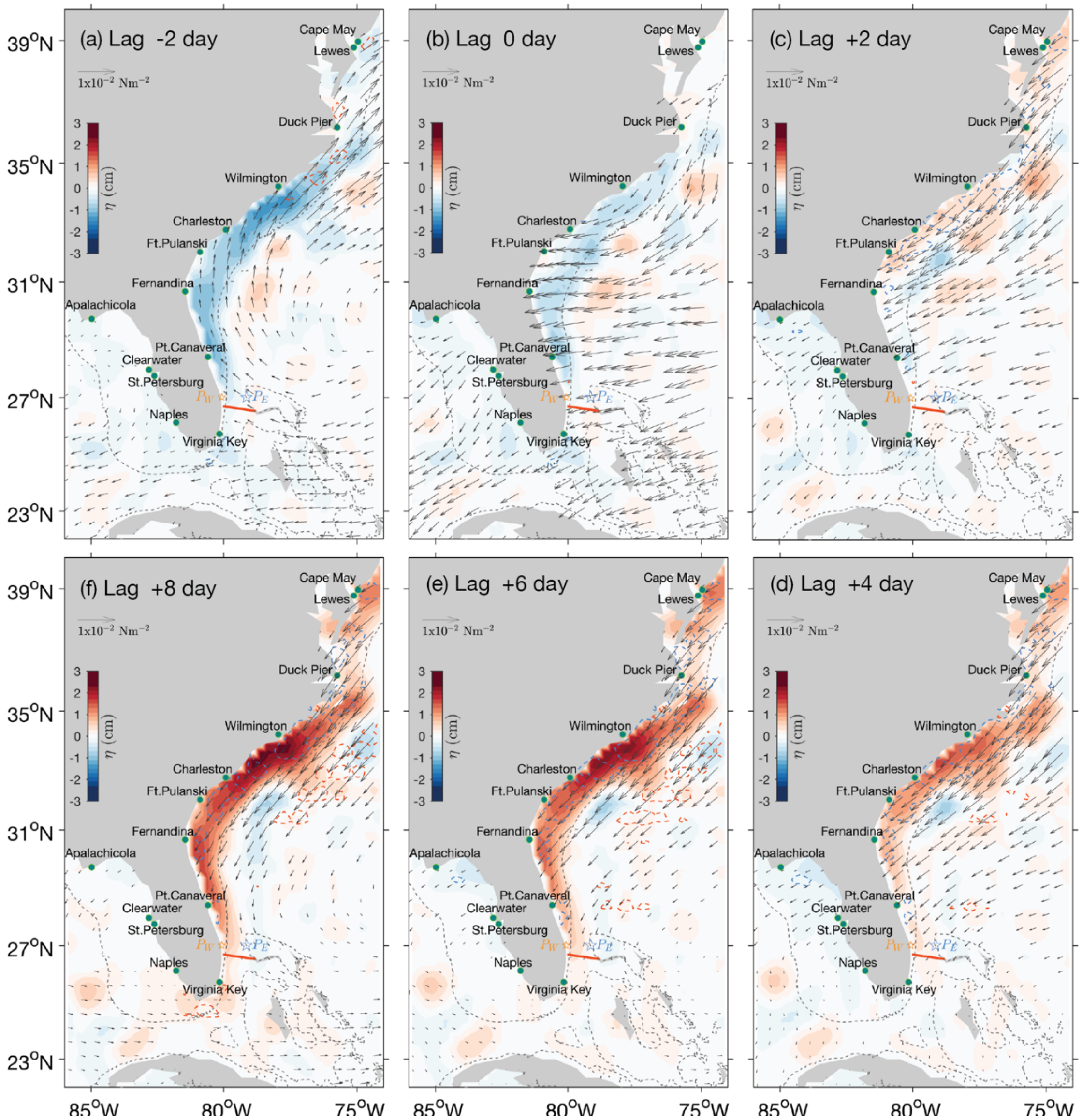

Figure 10. Time-evolution of the subseasonal variations of η (color shading), wind stress (arrows), and Ekman divergence (blue dashed contours) and convergence (red dashed contours), regressed against the principal component of the leading CEOF mode of the subseasonal coastal η data at tide gauges (green dots) along the U.S. East and Gulf Coast. The regressed values are scaled to one standard deviation of the principal component. Omitted values do not exceed the 95% significance level. Blue contours denote a value of -10^{-5} m s^{-1}, while the red ones indicate the opposite sign. Black dashed contours indicate an isobath of 200 m.

In-situ observations reveal the main characteristics of subseasonal variability in the Florida Straits and along the U.S. East and Gulf Coast. The observations also provide insights into coastal-trapped waves as an energy source for the subseasonal variability. To further illustrate the relationship between the observed subseasonal variability and coastal-trapped waves over the broader North Atlantic Ocean and probe the generating mechanisms of the waves, we next regress the subseasonal satellite-derived atmospheric and oceanic parameters onto the principal component of the leading CEOF mode of the subseasonal coastal η data.

Regressed η illustrates a spatial pattern reminiscent of coastal-trapped waves whose most robust signature is confined between the coastline and an isobar of 200 m (Fig. 10). The time evolution of the regressed η pattern demonstrates that elevated sea level anomaly hugging the coastline propagates towards the Gulf of Mexico via the Florida Straits. It takes about 3 - 4 days for the subseasonal coastal-trapped waves to transmit the η signal along the coast extending from Cape May to Virginia Key (Fig. 10b-f).

Based on regressed τ, it appears that the observed subseasonal coastal-trapped waves are a transient response to a change in the prevailing subseasonal wind field over the continental shelf region. An initial pattern of suppressed η turns into an elevated η pattern following an alongshore wind reversal from southwesterly to northeasterly roughly along the Southern Mid-Atlantic Bight and Carolina coast (Fig. 10a-c).

The southwesterly coastal τ is part of a subseasonal anticyclonic wind field over the interior of the subtropical North Atlantic (Fig. 11a). At lag 0, while subseasonal sea level anomaly along the U.S. East and Gulf Coast is suppressed, the wind is either northeasterly parallel with or into the coast, a wind condition that is not favorable for the suppressed η (Fig. 10b). Within the next two days, the northeasterly winds build up along the coast extending from Cape May to Fernandina beach and lead to areas of Ekman transport divergence off the coast, which coincide with the emergence of elevated η (Fig. 10c). As the winds intensify, subseasonal sea level anomaly continues to increase as well as propagate equatorward along the coast through the next couple of days (Fig. 10d-f). The intensification of the northeasterly coincides with the weakening of the anticyclonic wind over the basin interior (Fig. 11b).

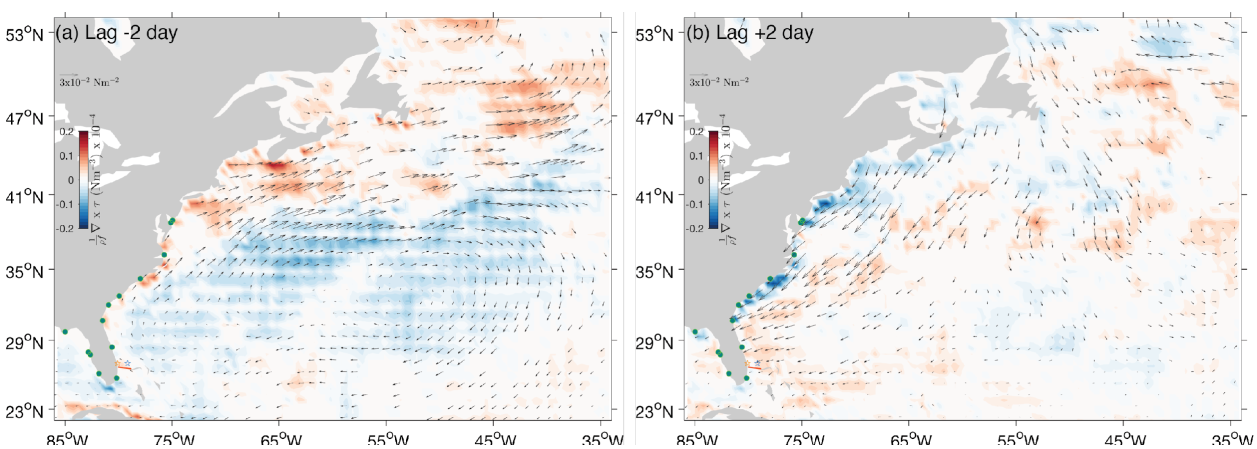

Figure 11. Time-evolution of the η (color shading), wind stress (arrows), and Ekman divergence (blue dashed contours) and convergence (red dashed contours) subseasonal variations regressed against the first principal component of the complex EOF of the subseasonal η data at tide gauge (green dots) along the U.S. East and Gulf Coast. The regressed values are scaled to one standard

deviation of the principal component, with omitted values below a 95% significance level. Blue contours denote a value of -10^{-5} ms^{-1}, while the red ones indicate the opposite sign. Black dashed contours indicate an isobath of 200 m.

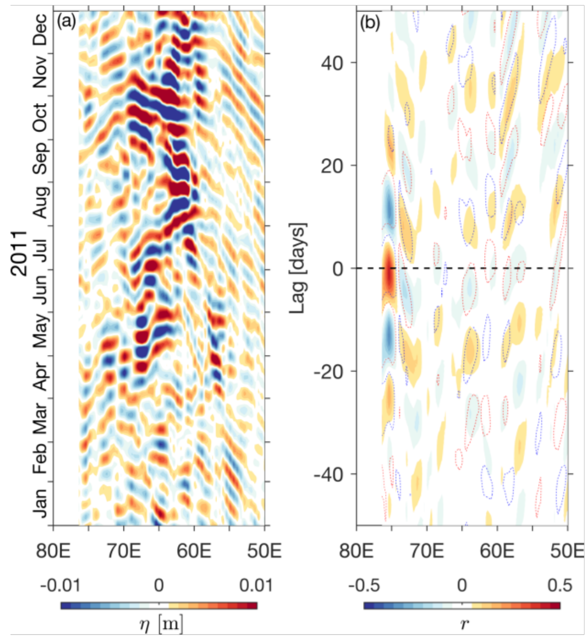

Figure 12. (a) A longitude-time plot of the subseasonal variability of satellite η averaged within a band of latitudes between 35 – 37°N in 2011. (b) The lagged correlation coefficients between the subseasonal altimetry η data averaged at latitudes between 35 – 37°N and the subseasonal coastal η data at Duck Pier (color shading) and the subseasonal FC transport estimates (dashed contours). The data used to compute the coefficients are between 2001 - 2019. Dashed red contours denote positive correlation values, while blue contours indicate negative correlations.

Many studies have proposed baroclinic Rossby waves originating from the interior of the North Atlantic as a source for the FC variability, particularly for seasonal and longer variations [e.g., *Domingues et al.*, 2016; *Calafat et al.,* 2018]. Once impinging upon the U.S. East Coast, the large and low-frequency waves partially turn into coastal-trapped waves, whose energy penetrates the Florida Straits and perturbs the mean flow therein.

To test whether long Rossby wave signals from the interior affect coastal sea level anomaly on subseasonal timescales, we analyzed subseasonal η at different longitudes within a band of latitudes between 35 - 37°N. A longitude-time plot of a subset of the subseasonal η data averaged within the latitude band illustrates a complex pattern of zonal propagation, with westward transmissions expected from Rossby waves being a dominant feature to the east of 70°E (Fig. 12a). Between the coast and 70°E, however, eastward phase propagation is more pronounced, likely a zonal projection of subseasonal eddy motions advected by the Gulf Stream. In general, the complex pattern of zonal propagation is evident in the subseasonal η data throughout the observational period (not shown).

Corroborating the inference from the hovmöller plot of the subseasonal η data at latitudes between 35 - 37°N (Fig. 12a), neither the FC transport estimates in the Florida Straits nor the tide gauge η data at Duck Pier (36°N) demonstrate a lagged correlation pattern indicative of Rossby waves as a facilitator connecting subseasonal signals in the interior and that along the U.S. East and Gulf Coast (Fig. 12b). A hovmöller plot of the lagged correlation of the tide gauge and satellite η on subseasonal timescales indicates that coastal sea level anomaly correlates to satellite sea level anomaly within about 500 - 700 km from the coast. The correlation shows a slanted pattern to the east, suggesting eastward phase propagation, not westward propagation expected from Rossby waves.

6. Discussion

We have described the main characteristics and plausible mechanisms of the energetic FC transport subseasonal variability in the Florida Straits. Our observations demonstrate that wind-forced coastally trapped waves originating along the Southern Mid-Atlantic Bight coast govern most of the subseasonal variances of the FC volume transport and the cross-stream pressure difference in the Florida Straits and sea level anomaly along the U.S. East and Gulf Coast.

Subseasonal variability constitutes a significant fraction of the total variance of the FC transport. The total percentage of the FC transport subseasonal variance is 37%, larger than that of the transport synoptic, seasonal, and interannual variances combined. Relative to the non-seasonal variances of the 20-day low-pass filtered FC transport anomalies, the subseasonal variance percentage increases to 62%. Similar to what is observed in the FC transport, subseasonal variability significantly contributes to the cross-stream pressure gradient changes, with its most robust signature on the west side of the Florida Straits.

The FC transport and the cross-stream pressure gradient are in geostrophic equilibrium on the subseasonal period band, implying decreased westward pressure gradient corresponds with reduced FC transport and vice versa. The pressure gradient subseasonal variability explains 50% of the FC transport subseasonal variance by assuming a linear relationship. The percentage increases to 70% when considering the data through September – November only. For comparison, the total pressure gradient variability accounts for about 55% of the total FC transport variance [*Meinen et al.*, 2021].

We argue that the contribution of local wind forcing to the Florida Straits subseasonal variability appears to be minor. Only 5% of the FC transport and the cross-stream pressure gradient variations correlate with local winds on the subseasonal period band. In contrast, *Schott et al.* [1988], supported by a frictional model result, suggested that the FC transport variances in the period range of 2 - 100 days respond to the local along-channel winds in the Florida Straits. However, the FC variability well simulated by their model mainly varies with timescales of 15 days and shorter (see Fig. 12a of *Schott et al.* [1988]), consistent with other studies demonstrating coupling between the FC transport and local winds on synoptic timescales, instead of subseasonal timescales [e.g., *Lee and Williams*, 1988].

While local winds appear insignificant, the subseasonal variations of the FC transport and the sea level anomaly between Cape May in New Jersey and Apalachicola in Florida exhibit a statistically significant correlation with $r^2 > 0.2$ in general, indicative of a remote source of the subseasonal variability observed in the Florida Straits. The coastal η data, from an array of tide gauges between Cape May and Apalachicola, demonstrate propagating subseasonal signals. About 61% of the coastal η subseasonal variance, isolated using the leading CEOF mode of the subseasonal coastal η data, demonstrates subseasonal coastal-trapped waves along the U.S. East and Gulf Coast.

When regressed against the principal component of the leading CEOF mode, subseasonal coastal η illustrates the spatial and temporal changes of subseasonal coastal-trapped waves. The regressed η at different tide gauges shows transmission of the subseasonal waves covering a wave path between Cape May and Port Isabel within 15 days, with the waves traveling faster along the U.S. East Coast for unknown reasons. For example, the wave phase speed is about 5.3 m s^{-1} between Cape May and Virginia Key along the East Coast, while it is 1.5 m s^{-1} between Virginia Key and Apalachicola along the Gulf Coast. These phase speed estimates agree with that inferred from the observed dispersion relation for subseasonal Kelvin waves, determined from a coherence analysis of subseasonal η at multiple pairs of tide gauges along the East and Gulf Coast. On average, the subseasonal mode propagates towards the Gulf of Mexico with a phase speed of 2.5 ± 0.4 m s^{-1}.

In the Florida Straits, subseasonal coastal-trapped waves markedly affect the FC transport. The regressed η and FC transport show that a subseasonal coastal-trapped wave pulse with an amplitude of 5 cm at Port Canaveral exerts a 1 Sv change in the FC transport. The average wave amplitude could be as high as 15 cm for extreme cases, and it may modulate the FC transport on average by 2.6 Sv, comparable to the standard deviation of the total FC transport variability. We note that the average amplitude of the extreme subseasonal waves is commensurate with the global average sea-level rise over the 20th century of about 16 cm [*Calafat et al.*, 2018].

A geostrophic balance between the FC transport and the cross-stream pressure gradient or east-west pressure difference is evident during subseasonal wave passage, with P_W controlling the pressure gradient change. The minimum P_E response is consistent with the zonal structure of the Kelvin wave pressure, which decays away from the Florida coast with a scale of about 27 km in the Florida Straits at 27ºN. *Mooers et al.* [2005] reported a similar decay scale of 25 km inferred from the zonal structure of the model FC throughout a strong cold front-forced coastal trapped wave event in the Florida Straits.

The stratification frequency and bottom topography across the Florida Straits at 27ºN indicate that the properties of Kelvin waves may explain the observed subseasonal coastal-trapped waves. A normal mode decomposition of the buoyancy frequency yields a phase speed of 1.8 m s^{-1} for the first baroclinic Kelvin wave mode, identical with that inferred from the observed dispersion diagram for the subseasonal η data at Port Canaveral and Virginia Key. Moreover, the baroclinic Rossby deformation radius is on average five times the cross-shelf scale of the bottom topography along 27ºN in the Florida Straits, implying a Kelvin wave prerequisite of near-vertical sidewall condition.

Subseasonal coastal-trapped wave energy substantially dissipates along the Gulf of Mexico coast. The regressed coastal η indicates that the observed subseasonal wave amplitude rapidly decreases between the Florida Straits and Port Isabel. Determining the root cause of the wave damping is beyond the scope of this study, but interactions with coastal and bottom topography and background mean flow might be a factor. As subseasonal waves propagate equatorward against strong background currents, such as the Gulf Stream and Loop Current, and along complex coastal curvatures with variable cross-stream bottom topography, wave energy attenuation is expected.

Low-frequency Rossby waves from the eastern North Atlantic are not the main contributor to the dynamic origins of the observed subseasonal coastal-trapped waves in the Florida Straits. Instead, Ekman dynamics alongshore of the southern Mid-Atlantic Bight may account for the genesis of the subseasonal waves. The emergence of subseasonal alongshore winds off the New Jersey coast and subsequently the Carolina coast precede the onset of the subseasonal mode. Against the semipermanent North Atlantic subtropical anticyclonic winds, the Ekman convergence-favorable northeasterly winds induce elevated coastal η off Cape May on subseasonal timescales. Conversely, the opposite holds for the Ekman divergence-favorable southeasterly winds. The perturbed sea level anomaly progresses toward the Gulf of Mexico as a train of subseasonal coastal-trapped waves, modulating coastal sea level anomaly along the wave path and the Florida Current transport in the Florida Straits. Some numerical experiments to further explore the subseasonal waves' genesis and impact on ocean-atmosphere interaction are to be carried out for future studies.

The basin-wide wind field associated with the subseasonal alongshore winds exhibits a vortex-like structure over the subtropical North Atlantic. Time evolution of the regressed subseasonal τ over the North Atlantic illustrates a subtropical anticyclonic circulation that transitions into cyclonic and vice versa prior to and during the generation of the observed subseasonal coastal-trapped waves. The subseasonal anticyclonic and cyclonic winds might be a subseasonal component of the subtropical anticyclone typically referred to as the “Azores” or "Bermuda High," part of the global atmospheric circulation [*Davis et al.*, 1997]. The subtropical anticyclone attains its minimum intensity in October [*Sahsamanoglou*, 1990], which interestingly coincides with the subseasonal waves’ most active period as observed in the coastal sea level anomaly and FC transport. *Davis et al.* [1997] ascribe the weakening of the subtropical anticyclone through boreal autumn to its high-pressure center’s eastward migration [*Davis et al.*, 1997], which shows profound subseasonal variations [*Osman et al.*, 2021]. Any plausible interplays between intensified subseasonal wind and suppressed subtropical anticyclone in autumn are to be investigated.

7. Conclusions

We evaluated the characteristics and dynamical origins of the FC subseasonal variability between 20 - 100 days from a suite of in-situ and satellite measurements in the Florida Straits and the broader region in the North Atlantic during 2001 - 2019. Results obtained in this work show that subseasonal variability comprises 37% of the total variance of the FC volume transport. It is energetic through September - November and attains its maximum in October. In addition, we also found that alongshore wind-forced coastal-trapped waves originating in the southern Mid-Atlantic Bight are the primary driver of the subseasonal variations of the FC transport and the sea level anomaly between Cape May and Port Isabel along the U.S East and Gulf Coast. In contrast, the role of local winds over the Florida Straits and low-frequency Rossby waves from the eastern North Atlantic is insignificant on subseasonal time scales.

In the Florida Straits, we infer that the observed subseasonal coastal-trapped waves exhibit Kelvin wave characteristics expected from theory. First, the observed dispersion diagram signifies a non-dispersive relation for the first baroclinic Kelvin wave mode. Second, the waveinduced FC transport change of 1 Sv is in geostrophic balance with the cross-stream pressure difference of about 3.5 cm. The subseasonal mode may change the FC transport on average by 2.6 Sv for extreme cases, close to the standard deviation of the total FC transport variability. Third, the cross-stream pressure structure exponentially decays eastward from the Florida coast with a scale of 27 km, a function of the baroclinic Rossby deformation radius. Fourth, the deformation radius on average exceeds the cross-shelf scale by a factor of five, justifying a vertical sidewall approximation.

A subseasonal coastal-trapped wave pulse completes its cycle in 35 days. It propagates along a coastal waveguide between Cape May and Port Isabel within 15 days with an average phase speed of 2.5 ± 0.4 m s^{-1}. The subseasonal wave amplitude is up to 15 cm at Port Canaveral and rapidly decays as it transmits along the Gulf of Mexico coast. Only 20% of the wave energy remains along the Texas shelf coast.

Assessing implications of the subseasonal mode on coastal inundation along the U.S. East and Gulf Coast and ocean-atmosphere interactions along the Gulf Stream path and the broader subtropical North Atlantic region is of interest for future studies.

Acknowledgments

The authors acknowledge support from the NOAA Atlantic Oceanographic and Meteorological Laboratory. This research was carried out in part under the auspices of the Cooperative Institute for Marine and Atmospheric Studies, a Cooperative Institute of the University of Miami and the National Oceanic and Atmospheric Administration, cooperative agreement #NA20OAR4320472. DLV was also supported by NOAA's Climate Variability and Predictability program (grant number NA20OAR4310407) and by the AOML's Western Boundary Time Series project. Gratitude is extended to Dr. Greg Foltz for providing constructive comments on an earlier version of this manuscript. The FC transport estimates from cable voltages and altimetry can be downloaded via www.aoml.noaa.gov/phod/floridacurrent/, the pressure, LADCP, and dropsonde data are available at www.aoml.noaa.gov/phod/wbts/, and the XBT data are archived at https://www.aoml.noaa.gov/phod/goos/xbtscience/data.php. The satellite data can be obtained from http://marine.copernicus.eu/services-portfolio/access-to-products.

References

Baringer, M. O. N., and J. C. Larsen (2001), Sixteen years of Florida Current transport at 27 N, *Geophys Res Lett*, *28*(16), 3179-3182.

Beal, L. M., J. M. Hummon, E. Williams, O. B. Brown, W. Baringer, and E. J. Kearns (2008), Five years of Florida Current structure and transport from the Royal Caribbean Cruise Ship Explorer of the Seas, *Journal of Geophysical Research: Oceans*, *113*(C6).

Bentamy, A., K. Katsaros, W. Drennan, and E. Forde (2002), Daily surface wind fields produced by merged satellite data, *Gas Transfer at Water Surfaces*, *127*, 343-349.

Calafat, F. M., Wahl, T., Lindsten, F., Williams, J., & Frajka-Williams, E. (2018). Coherent modulation of the sea-level annual cycle in the United States by Atlantic Rossby waves. *Nature communications*, *9*(1), 1-13.

Caldwell, P. C., M. A. Merrifield, P. R. Thompson (2015), Sea level measured by tide gauges from global oceans — the Joint Archive for Sea Level holdings (NCEI Accession 0019568), Version 5.5, *NOAA National Centers for Environmental Information*, Dataset, doi:10.7289/V5V40S7W.

Cushman-Roisin, Benoit, and Jean-Marie Beckers (2011). *Introduction to geophysical fluid dynamics: physical and numerical aspects*. Academic press.

Czeschel, L., C. Eden, and R. J. Greatbatch (2012), On the driving mechanism of the annual cycle of the Florida Current transport, *J Phys Oceanogr*, *42*(5), 824-839.

Domingues, R., M. Baringer, and G. Goni (2016), Remote sources for year-to-year changes in the seasonality of the Florida Current transport, *Journal of Geophysical Research: Oceans*, *121*(10), 7547-7559, doi:https://doi.org/10.1002/2016JC012070.

Garcia, R. F., and C. S. Meinen (2014), Accuracy of Florida Current volume transport measurements at 27 N using multiple observational techniques, *J Atmos Ocean Tech*, *31*(5), 1169-1180.

Johns, W. E., and F. Schott (1987), Meandering and transport variations of the Florida Current, *J Phys Oceanogr*, *17*(8), 1128-1147.

Lau, William K-M., and Duane E. Waliser. *Intraseasonal variability in the atmosphere-ocean climate system*. Springer Science & Business Media, 2011.

Larsen, J.C., 1991. Transport measurements from in-service undersea telephone cables. IEEE J. Oceanic Eng. 16 (4), 313–318.

Larsen, J., and F. Smith (1992), Transport and heat flux of the Florida Current at 27 N derived from cross-stream voltages and profiling data: Theory and observations, *Philosophical Transactions of the Royal Society of London. Series A: Physical and Engineering Sciences*, *338*(1650), 169-236.

Lee, T. N., F. A. Schott, and R. Zantopp (1985), Florida Current: Low-Frequency Variability as Observed with Moored Current Meters during April 1982 to June 1983, *Science*, *227*(4684), 298-302.

Lee, T. N., and E. Williams (1988), Wind-Forced Transport Fluctuations of the Florida Current, *J Phys Oceanogr*, *18*(7), 937-946, doi:Doi 10.1175/1520-0485(1988)018<0937:Wftfot>2.0.Co;2.

Maloney, E. D., Chelton, D. B., & Esbensen, S. K. (2008). Subseasonal SST variability in the tropical eastern North Pacific during boreal summer. *Journal of Climate*, *21*(17), 4149-4167.

Meinen, C. S., M. O. Baringer, and R. F. Garcia (2010), Florida Current transport variability: An analysis of annual and longer-period signals, *Deep Sea Research Part I: Oceanographic Research Papers*, *57*(7), 835-846.

Meinen, C. S., R. H. Smith, and R. F. Garcia (2021), Evaluating pressure gauges as a potential future replacement for electromagnetic cable observations of the Florida Current transport at 27 degrees N, *J. Oper. Oceanogr.*, *14*(2), 166-176, doi:10.1080/1755876x.2020.1780757.

Molinari, R. L., W. D. Wilson, and K. Leaman (1985), Volume and Heat Transports of the Florida Current: April 1982 Through August 1983, *Science*, *227*(4684), 295-297, doi:10.1126/science.227.4684.295.

Mooers, C. N. K., Meinin, C. S., Baringer, M. O., Bang, I., Rhodes, R., Barron, C. N., & Bub, F. (2005). Cross validating ocean prediction and monitoring systems. *Eos, Transactions American Geophysical Union*, *86*(29), 269-273.

Percival, D. B., and A. T. Walden (1993), *Spectral analysis for physical applications*, Cambridge university press.

Rosenfeld, L. K., R. L. Molinari, and K. D. Leaman (1989), Observed and Modeled Annual Cycle of Transport in the Straits of Florida and East of Abaco-Island, the Bahamas (26.5-Degrees-N), *J Geophys Res-Oceans*, *94*(C4), 4867-4878, doi:10.1029/JC094iC04p04867.

Schott, F. A., S. A. Frisch, and J. C. Larsen (1986), Comparison of Surface Currents Measured by HF Doppler Radar in the Western Florida Straits during November 1983 to January 1984 and Florida Current Transports, *J Geophys Res-Oceans*, *91*(C7), 8451-8460, doi: 10.1029/JC091iC07p08451.

Schott, F. A., T. N. Lee, and R. Zantopp (1988), Variability of structure and transport of the Florida Current in the period range of days to seasonal, *J Phys Oceanogr*, *18*(9), 1209-1230.

Thomson, R. E., and W. J. Emery (2014), Chapter 5 - Time Series Analysis Methods, in *Data Analysis Methods in Physical Oceanography (Third Edition)*, edited by R. E. Thomson and W. J. Emery, pp. 425-591, Elsevier, Boston, doi:https://doi.org/10.1016/B978-0-12-387782-6.00005-3.

Volkov, D. L., R. Domingues, C. S. Meinen, R. Garcia, M. Baringer, G. Goni, and R. H. Smith (2020), Inferring Florida Current Volume Transport From Satellite Altimetry, *Journal of Geophysical Research: Oceans*, *125*(12), e2020JC016763, doi:https://doi.org/10.1029/2020JC016763.